Journal of ELECTRONIC MATERIALS, Vol. 50, No. 4, 2021
https://doi.org/10.1007/s11664-020-08366-6

ASIAN CONSORTIUM ACCMS–INTERNATIONAL CONFERENCE ICMG 2020

Optimization and Thermal Analysis of Fe_2O_3 Nanoparticles Embedded Myristic Acid-Lauric Acid Phase Change Material

MALVIKA SATISH,[1] SHARON SANTHOSH,[1] APURV YADAV,[1] SUJITH KALLURI,[2] and ASHA ANISH MADHAVAN[1,3]

1.—Department of Engineering, Amity University Dubai, Dubai, UAE. 2.—Department of Electronics and Communication Engineering, School of Engineering and Applied Sciences, SRM University-AP, Amaravati, Andhra Pradesh 522502, India. 3.—e-mail: ashaanish.madhavan@gmail.com

Phase change materials (PCM) are commonly utilized materials in latent heat energy storage systems. In the present study, Fe_2O_3 was incorporated into the eutectic mixture of myristic acid and lauric acid. The composites were prepared by a melting and mixing method. Fourier transform infrared spectroscopy and dynamic light scattering results revealed the physicochemical properties of the eutectic mixture. Thermal analysis was performed on the optimized PCM mixtures with various Fe_2O_3 loadings of 1 wt.%, 2 wt.%, 3 wt.%, 4 wt.%, and 5 wt.%. It is observed from the experimental results that the duration of melting and cooling rates for PCM composite with 4 wt.% Fe_2O_3 loadings was significantly improved, i.e., 85.72% and 78.31%, respectively, when compared to its pristine counterparts. These enhanced heating/cooling rates and thermal conductivity are attributed to the optimized impregnation of 4 wt.% Fe_2O_3 nanostructures into the eutectic mixture.

Key words: Phase change material, lauric acid–myristic acid, eutectic mixture, Fe_2O_3, heat transfer

INTRODUCTION

With the accelerated development and global trends of urbanization, there is no doubt that energy conservation is the need of the hour. Energy conservation is a twofold process. It can be achieved by limiting the amount of energy used for different purposes and/or by making use of energy more efficient. Financial, political, and environmental stability can be achieved by conscious use of resources by nations. For energy conservation in buildings and public facilities, thermal energy storage (TES) is an essential factor.

Latent heat thermal energy storage (LHTES) using phase change materials (PCMs) has recently gained much popularity. It is possible to attain high storage density in small volumes and compact size of systems using PCMs. Furthermore, they have the advantage of having a small range of temperatures to store and release thermal energy.[1] PCMs can be used as TES solutions in various fields. They have been extensively used in the cooling of electronic devices and electrical engines, spacecraft thermal systems, biomedical applications, storage and transport of temperature-sensitive commodities, etc. Apart from these applications, they can be implemented in buildings for the purpose ventilation, air-conditioning, and solar heating, to enhance recovery of waste heat and decrease fluctuations in indoor temperature.[2–5]

Inorganic salt hydrates, paraffin waxes, and fatty acids have been researched broadly to be used for various commercial applications. Among these, fatty acids have shown promising behaviors of high latent heat capacity, congruent melting behavior, thermal stability, non-toxicity, and little volume change on repeated cycling. Moreover, they are

(Received May 8, 2020; accepted July 28, 2020; published online August 11, 2020)

economical and can be easily extracted from animal and vegetable oils.[6]

A few limitations, however, hinder the utilization of fatty acids. Two major drawbacks include poor thermal conductivity and a fairly high melting temperature. Rather than making use of pristine PCMs, binary and ternary eutectic mixtures of fatty acids can be developed to modify the melting and solidification temperatures in accordance with the specific application and climatic needs.[7] There have been many approaches to combat the problem of low thermal conductivity. These include inserting concentrated fins, incorporating porous structure materials, macro- and micro-encapsulation techniques, and the addition of nanoparticles of high thermal conductivity.[8–16]

For this research, metal oxide nanoparticles of iron oxide have been integrated with the eutectic mixture of myristic acid and lauric acid to form a suitable composite with moderately high thermal conductivity. A novel eutectic mixture of nano-enhanced PCM (NEPCM) has been developed. This work focuses to compliment a study on the preparation and characterization of a binary eutectic mixture of fatty acid incorporated with nanoparticles of iron oxide. A combination of myristic acid and lauric acid is preferred, given their similar chemical structure and relatively low phase change temperature. The thermal and physicochemical properties of the composite PCM were characterized by Fourier transformation infrared spectroscopy (FT-IR), thermogravimetric analysis–differential scanning calorimetry (TGA–DSC), and dynamic light scattering (DLS).

MATERIALS AND METHODS

Materials

Myristic acid (MA) of 99% purity and lauric acid (LA) were purchased from Amrut Industrial Products, India. Iron oxide was purchased from Research-Lab Fine Chem Industries, India. The iron oxide was of extra purity with an assay of 95.0–98.0%.

Preparation of MA-LA Binary Eutectic Mixtures

Firstly, 10 g of MA-LA binary eutectic mixture was prepared in different concentration ratios by weight of MA and LA, respectively (100:0, 80:20, 60:40, 50:50, 40:60, 20:80). Then, 4 wt.% of extra-pure iron oxide was added as this composite showed the best results when tested against pristine MA and pristine LA. Fe_2O_3 was manually added and stirred until completely dispersed in the mixture, and the mixture was subsequently heated and cooled to record the melting and cooling curves for thermal analysis. The samples were placed in a hot water bath and the changing temperatures of the PCMs were recorded every 30 s using a Thermo Pro TP-17 dual probe digital thermometer as shown in Fig. 1. The samples were heated to 70°C and then cooled by convection to room temperature of 25°C. The solidification temperatures were also measured every 30 s for accuracy.

RESULTS AND DISCUSSION

The prepared compositions of the eutectic mixtures were thoroughly tested for their physicochemical and thermal properties. The optimized proportion of the eutectic mixtures of MA and LA without and with Fe_2O_3 (IO) nanostructure, represented by 50M + 50L and 50M + 50L + 4% IO, respectively, were characterized using FT-IR. Figure 2 represents the FT-IR spectra of 50M + 50L and 50M + 50L + 4% IO compositions. The various peaks in the spectra represent the significance of different functional groups. Thus, the resulted spectrum of 50M + 50L + 4% IO reveals the efficient embedment of IO with MA and LA eutectic mixture. The multiple peaks shown below 600 cm^{-1} are attributed to the Fe–O stretching bands. Two characteristic bands of hematite at 471 cm^{-1} and 548 cm^{-1} are observed.[17,18] The bands at 420 cm^{-1}, 490 cm^{-1} are due to the Fe–O stretching vibrational modes.[19,20] The peaks around 1417 cm^{-1} and 2851 cm^{-1} are corresponding to the carbonyl C–H symmetric stretching in MA/LA. These results confirm that the IO has been dispersed effectively in the eutectic mixture of MA and LA. DLS characterization was performed to identify the particle size of IO nanostructures that are used in this work. The IO samples were dispersed in ethanol and

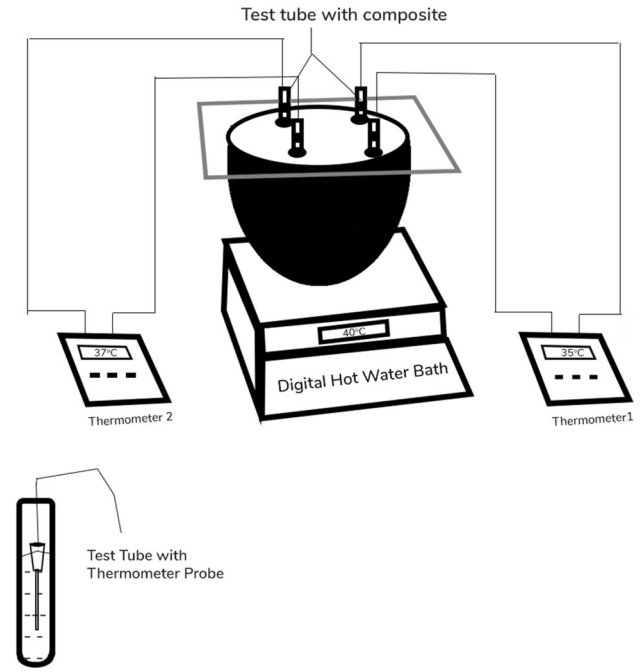

Fig. 1. Schematic representation of experimental setup to prepare eutectic mixtures.

analyzed by DLS, which revealed the particle size of IO nanoparticles as 84.5 ± 5 nm.

To achieve better chemical and thermal stability of eutectic-based PCMs, there should be systematic optimization among the constituents in the eutectic mixture and foreign dopants. In this work, the NEPCM was carefully obtained by the initial preparation of eutectic mixtures with the various proportions of MA and LA, i.e., 80 wt.% MA + 20 wt.% LA (represented as 80M + 20L), 60M + 40L, 50M + 50L, 40M + 60L, and 20M + 80L without a foreign dopant, IO. To judge the optimized proportion of MA and LA eutectic mixture suitable for PCMs, the thermal studies such as melting rate and cooling rate tests have been performed on the pristine and various eutectic mixture proportions (mentioned above). These melting and cooling tests were conducted using the experimental setup shown in Fig. 1. Figure 3 shows the melting rate and cooling rate curves of MA and LA eutectic mixtures of different proportions, and Table I represents their respective melting and cooling rates. From these curves, we can understand that the ratio of 50 wt.% MA and 50 wt.% LA shows the highest heat transfer rate with a value of 36.66% (see Table I, Fig. 3a), whereas 80 wt.% MA and 20 wt.% LA mixture has the lowest heat transfer rate of 26.66%. These PCM composites started at an initial average ambient temperature of 23°C. The temperatures were increased beyond their phase change temperatures to an average temperature of 65°C. On the other hand, the cooling rate curves represented in Fig. 3b also show that the same proportion of eutectic mixture, i.e., 50 wt.% MA and 50 wt.% LA, exhibits the highest heat transfer rate, with a value of 65.17%, with the 80 wt.% MA and 20 wt.% LA mixture being the lowest (see Table I). The nonuniformity in the heating/cooling rates could be associated with the thermal and chemical stabilities of the MA and LA in the various proportions of the eutectic mixture. There is a relationship between the temperature of cooling/heating and their storage capacity. Further, with respect to change in the proportion of eutectic, the storage density of the eutectic changes, leading to nonuniform heat transfer rates.[21] These PCM composites started at an initial elevated temperature of 65°C. The temperatures were increased beyond their phase change temperatures and then cooled to a room temperature of 25°C. The better heat transfer rates in the 50 wt.% MA and 50 wt.% LA mixture could be attributed to the good intermixing of the eutectic at that proportion, which could result in a low melting temperature to the greatest extent possible. In addition, the thermochemical stability and phase change feasibility of the eutectic associated with the chemically relevant MA and LA structures at the optimized proportion (50 wt.% MA + 50 wt.% LA) together with the optimized impregnation of Fe_2O_3 nanostructures into eutectic is also responsible for better melting and cooling rates (discussed in further section).

Nonetheless, the above optimization is without foreign dopant, i.e., Fe_2O_3 (IO), in the eutectic. There could be variation in these heat transfer rates when the dopant (IO) is embedded into the eutectic mixture, because of possible changes in the heat

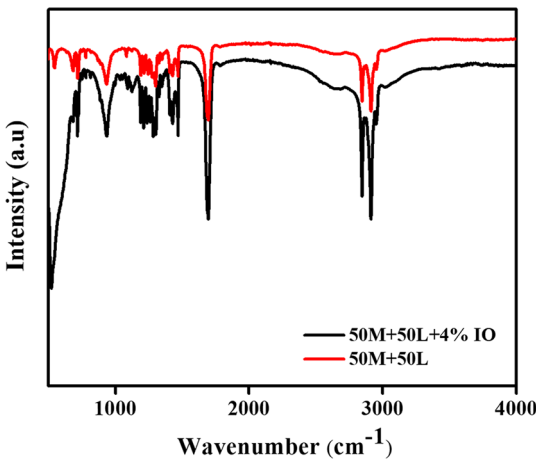

Fig. 2. FTIR spectra of myristic acid and lauric acid eutectic mixture without and with 4 wt.% Fe_2O_3.

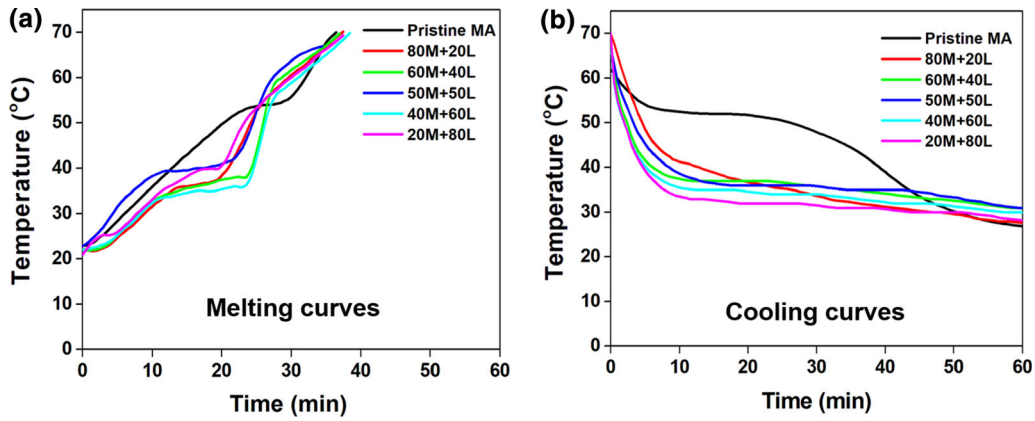

Fig. 3. (a) and (b): Melting and cooling curves during thermal analysis of eutectic mixtures with various proportions of myristic acid and lauric acid without Fe_2O_3.

transfer dynamics. In this regard, thermal melting and cooling rate studies have been performed for the eutectic samples of various MA and LA proportions with the different proportions of dopants, i.e., 1 wt.% IO, 2 wt.% IO, 3 wt.% IO, and 4 wt.% IO. The melting curves (see Fig. 4a, b, c, and d) for various concentrations of MA and LA eutectic mixtures with 1 wt.% IO, 2 wt.% IO, 3 wt.% IO, and 4 wt.% IO are plotted in the graphs. From these values, we can understand that the ratio of 50 wt.% MA and 50 wt.% LA eutectic mixture with 4 wt.% IO shows the highest heat transfer rate with a value of 85.71% (see Table II). These PCM composites started at an initial average ambient temperature of 23°C. The temperatures were increased beyond their phase change temperatures and were heated up to an average temperature of 65°C. Interestingly, the same 50 wt.% MA and 50 wt.% LA eutectic mixture showed a high heat transfer rate of around 78.31% when the proportion of IO was 3–4 wt.% during the cooling test of the mentioned samples (Fig. 5 and Table III). The cooling heat transfer rates were very similar, at 3 wt.% IO and 4 wt.% IO, and the melting heat transfer rate was high at 4 wt.% of IO (see Table III). Hence, the optimized proportion of IO in the 50 wt.% MA and 50 wt.% LA eutectic mixture was 4 wt.%, and the resultant composite 50 wt.% MA + 50 wt.% LA + 4 wt.% IO was nano-enhanced PCM. The improved heating/cooling heat transfer rates of the nano-enhanced

Table I. Melting and cooling rates of eutectic mixtures with various proportions of myristic acid and lauric acid

Ratio of eutectic mixtures	Melting rate (%)	Cooling rate (%)
80 wt.% MA + 20 wt.% LA	26.66	63.30
60 wt.% MA + 40 wt.% LA	37.93	64.44
50 wt.% MA + 50 wt.% LA	36.66	65.17
40 wt.% MA + 60 wt.% LA	33.33	62.13
20 wt.% MA + 80 wt.% LA	29.03	64.83

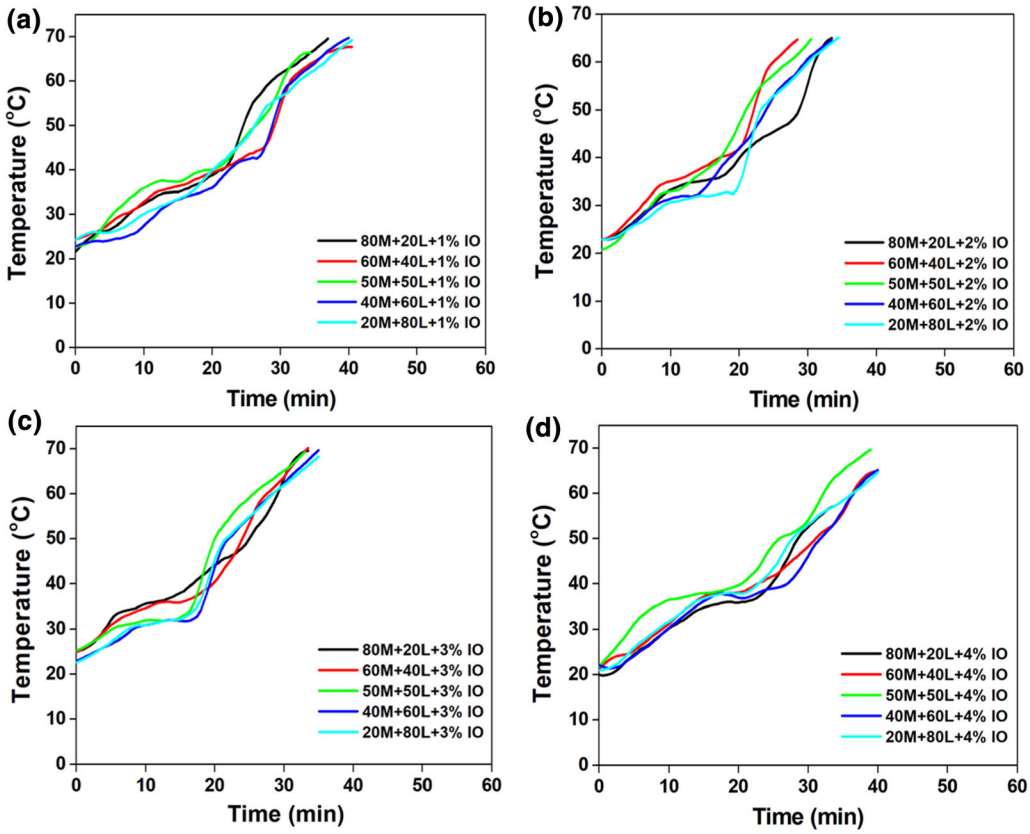

Fig. 4. Melting curves during thermal analysis of eutectic mixtures with various proportion of myristic acid and lauric acid with impregnation of (a) 1 wt.% Fe_2O_3, (b) 2 wt.% Fe_2O_3, (c) 3 wt.% Fe_2O_3, and (d) 4 wt.% Fe_2O_3.

Table II. Melting rates of eutectic mixtures of myristic acid and lauric acid with various proportions of Fe_2O_3 nanostructure

Ratio of eutectic mixtures	1 wt.% Fe_2O_3 (%)	2 wt.% Fe_2O_3 (%)	3 wt.% Fe_2O_3 (%)	4 wt.% Fe_2O_3 (%)
80 wt.% M + 20 wt.% L	30.76	40.90	52.07	58.62
60 wt.% M + 40 wt.% L	38.46	42.10	56.25	56.66
50 wt.% M + 50 wt.% L	46.42	44.44	72.22	85.71
40 wt.% M + 60 wt.% L	32.14	47.36	54.54	52.94
20 wt.% M + 80 wt.% L	29.62	41.37	52.63	59.25

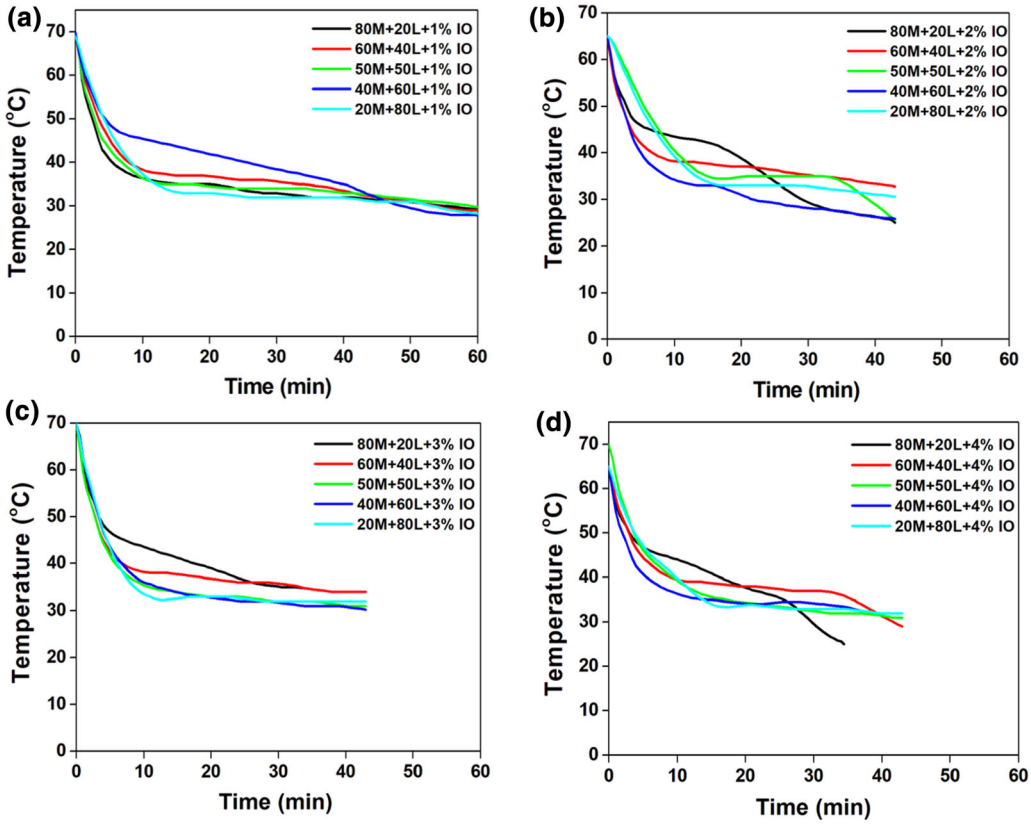

Fig. 5. Cooling curves during thermal analysis of eutectic mixtures with various proportions of myristic acid and lauric acid with impregnation of (a) 1 wt.% Fe_2O_3, (b) 2 wt.% Fe_2O_3, (c) 3 wt.% Fe_2O_3, and (d) 4 wt.% Fe_2O_3.

Table III. Cooling rates of eutectic mixtures of myristic acid and lauric acid with various proportions of Fe_2O_3 nanostructure

Ratio of eutectic mixtures	1 wt.% Fe_2O_3 (%)	2 wt.% Fe_2O_3 (%)	3 wt.% Fe_2O_3 (%)	4 wt.% Fe_2O_3 (%)
80 wt.% M + 20 wt.% L	70.21	71.51	73.83	76.38
60 wt.% M + 40 wt.% L	73.70	75.60	76.30	78.17
50 wt.% M + 50 wt.% L	70.15	75.19	79.35	78.31
40 wt.% M + 60 wt.% L	70.32	71.58	75.31	77.46
20 wt.% M + 80 wt.% L	71.96	76.78	78.56	79.68

PCM are attributed to the doping/intermixing of the appropriate proportion of IO (4 wt.%) in the eutectic, and thus the enhanced the thermal conductivity of the PCM. The incorporation of IO nanoparticles in the MA and LA eutectic leads to the reduction of phase change transition temperature when compared to that of un-doped eutectic samples. This is attributed to the increased surface area of the IO

nanoparticles. The same is evident from the DSC studies in this work and consistent with results reported elsewhere.[22]

Besides, the thermal tolerance of the prepared samples is one of the key features for efficient PCMs. Thus, the prepared eutectic mixtures without and with 4 wt.% IO were subjected to the TGA test, and corresponding thermograms are represented in Fig. 6. All the tested samples show the thermal degradation around the temperature of 250–300°C. The thermal degradation of pristine MA, LA, and MA + LA is early when compared to that of the MA + LA + 4 wt.% IO sample. The delay in the thermal degradation of the eutectic mixture with 4 wt.% IO corresponds to the thermal retardant effect of the incorporated IO nanoparticles.[23] The char residues are 2.58% and 7.14% for samples without and with 4 wt.% IO in 50 wt.% MA + 50 wt.% LA eutectic, respectively. The variation in the char residue values represents the presence of IO nanoparticles in the PCM. Furthermore, the higher heat transfer rates observed can be attributed to the path of high interfacial thermal conductance provided by the incorporation of IO nanoparticles in the PCM. The conduction is the dominating mechanism of heat transfer till the composite changes its phase to the liquid state. Although convection dominates in the liquid state, the interfacial thermal conductance is one order lower than that in a solid state.[24] Therefore, the effect of IO nanoparticles in enhancing the heat transfer is significant. These results further confirm the thermal stability and no degradation of samples below 100–150°C, which is the usual application range of a PCM.

On the other hand, DSC analysis was performed to understand the thermal storage capacity of the prepared samples. Table IV presents the phase transition temperature and latent heat values of the eutectic samples with and without 4 wt.% IO. From Fig. 7 and Table IV, it can be implied that the thermal storage capacity of MA + LA and MA + LA + 4 wt.% IO is 167.31 ± 8.14 and 153.56 ± 4.83 J g^{-1}, respectively. The melting peak temperature of MA + LA + 4 wt.% IO is higher (41.81°C) than that of MA + LA (40.62°C). The slight variation could be due to the proportionate doping of IO nano-particulates into the optimized eutectic mixture. These thermal studies confirm that the MA + LA + 4 wt.% IO eutectic mixture is an optimized and appealing candidate as a nano-enhanced PCM.

CONCLUSION

In summary, a binary eutectic mixture of myristic acid and lauric acid was synthesized and incorporated with iron oxide through dispersion in various concentration ratios. These composite mixtures were then subjected to melt/freeze cycles through which analysis of the heat transfer rates was obtained. The study showed that the incorporation

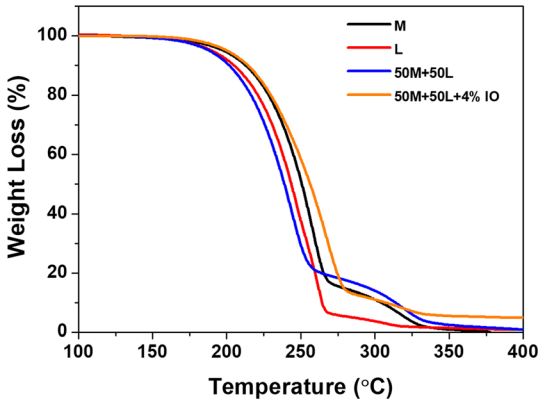

Fig. 6. TGA thermograms of myristic acid, lauric acid, and eutectic mixtures of myristic acid and lauric acid without and with 4 wt.% Fe_2O_3.

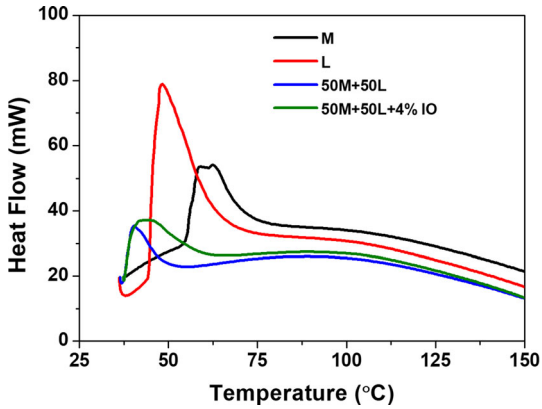

Fig. 7. DSC curves of myristic acid, lauric acid, and eutectic mixtures of myristic acid and lauric acid without and with 4 wt.% Fe_2O_3.

Table IV. Latent heat values of myristic acid, lauric acid, and eutectic mixtures of myristic acid and lauric acid without and with Fe_2O_3

Eutectic mixture	Onset temperature (°C)	Peak temperature (°C)	Latent heat (J/g)
M	54.46 ± 0.30	58.56 ± 0.30	197.87 ± 13.12
L	44.38 ± 0.30	48.17 ± 0.30	165.79 ± 11.36
50 wt.% M + 50 wt.% L	37.12 ± 0.30	40.62 ± 0.30	167.31 ± 8.14
50 wt.% M + 50 wt.% L + 4 wt.% Fe_2O_3	37.47 ± 0.30	41.81 ± 0.30	153.56 ± 4.83

of iron oxide nanoparticles led to improved thermal conductivity through enhanced heat transfer rates, which was confirmed by the various characterization techniques conducted and presented in this paper. The best heat transfer rate was observed for 50 wt.% MA + 50 wt.% LA incorporated with 4 wt.% iron oxide. The test showed good thermal stability without any chemical interaction. Other added advantages are the low cost of the raw materials, which altogether cost an average of INR 500. This indicates that this eutectic composite mixture is a potential candidate for highly efficient thermal energy storage systems under controlled conditions.

ACKNOWLEDGMENTS

The authors are grateful to the administration and management of Amity University Dubai, UAE, for providing infrastructure and other support for conducting the research.

CONFLICT OF INTEREST

The authors declare that they have no conflict of interest.

REFERENCES

1. C. Alkan, A. Sarı, and A. Karaipekli, *Energy Convers. Manag.* 52, 687 (2011).
2. A.M. Khudhair and M.M. Farid, *Energy Convers. Manag.* 45, 263 (2004).
3. M. Kenisarin and K. Mahkamov, *Renew. Sust. Energy Rev.* 11, 1913 (2007).
4. A.M. Borreguero, M.V. Sánchez, M.L. Sánchez-Silva, M.S. Carmona, and J.F. Rodríguez, in *IIR Proceedings Series 'Refrigeration Science and Technology* (2010), pp. 29–36.
5. X. Zhang, S. Yu, M. Yu, and Y. Lin, Y. *Appl. Therm. Eng.* 31, 3736 (2011).
6. A. Karaipekli and A. Sari, *Sol. Energy* 83, 323 (2009).
7. A. Sari, *Appl. Therm. Eng.* 25, 2100 (2005).
8. J.M. Khodadadi and S.F. Hosseinizadeh, *Int. Commun. Heat Mass Transf.* 34, 534 (2007).
9. M. Sheikholeslami, R. Haq, A. Shafee, and Z. Li, *Int. J. Heat Mass Transf.* 130, 322 (2019).
10. J. Wang, H. Xie, Z. Guo, L. Guan, and Y. Li, *Appl. Therm. Eng.* 73, 1541 (2014).
11. S. Santhosh and A.A. Madhavan, in *2019 Advances in Science and Engineering Technology International Conferences (ASET)* (2019), pp. 1–5.
12. W. Jifen, X. Huaqing, and Y. Li, *J. Nanosci. Nanotechnol.* 15, 3276 (2015).
13. A.B. Rezaie and M. Montazer, *Appl. Energy* 262, 114501 (2020).
14. J. Singh, J.R. Vennapusa, and S. Chattopadhyay, *Carbohydr. Polym.* 229, 115531 (2020).
15. M. Zhao, X. Zhang, and X. Kong, *Renew. Energy* 147, 374 (2020).
16. Y. Fang, L. Huang, X. Liang, S. Wang, H. Wei, X. Gao, and Z. Zhang, *Sol. Energy Mater. Sol. Cells* 206, 110257 (2020).
17. J. Serna, M. Ocana, and J.E. Iglesias, *J. Phys. C, Solid State Phys.* 20, 473 (1987).
18. Y. Wang, A. Muramatsu, and T. Sugimoto, *Colloids Surf. A, Physicochem. Eng. Aspects* 134, 281 (1998).
19. R. Sharma, S. Lamba, and S.A. Poorni, *J. Phys. D Appl. Phys.* 38, 3354 (2005).
20. R. Suresh, R. Prabu, A. Vijayaraj, K. Giribabu, A. Stephen, and V. Narayanan, *Synth. React. Inorg. Metal-Org. Nano-Met. Chem.* 42, 303 (2012).
21. M. Kamimoto, T. Tanaka, T. Tani, and T. Horigome, *Sol. Energy* 24, 581 (1980).
22. S.I. Golestaneh, G. Karimi, A. Babapoor, and F. Torabi, *Appl. Energy* 212, 552 (2018).
23. R. Sharma, P. Ganesan, V. Tyagi, H. Metselaar, and S. Sandaran, *Appl. Therm. Eng.* 99, 1254 (2016).
24. S. Harish, D. Orejon, Y. Takata, and M. Kohno, *Appl. Therm. Eng.* 114, 1240 (2017).